Electrochemical and Solid-State Letters, **11** (9) K89-K92 (2008)
1099-0062/2008/11(9)/K89/4/$23.00 © The Electrochemical Society

Atomic Layer Deposition of Ru Nanocrystals with a Tunable Density and Size for Charge Storage Memory Device Application

Sung-Soo Yim,[a] Do-Joong Lee,[a] Ki-Su Kim,[a,c] Moon-Sang Lee,[a,d] Soo-Hyun Kim,[b,*] and Ki-Bum Kim[a,*,z]

[a]*Department of Materials Science and Engineering, Seoul National University, Seoul 151-742, Korea*
[b]*School of Materials Science and Engineering, Yeungnam University, Gyeongsan, Gyeoungsangbuk-do 712-749, Korea*

We propose a deposition method capable of independently controlling the spatial density and average size of Ru nanocrystals by using both plasma-enhanced and thermal atomic layer deposition (ALD). Plasma-enhanced ALD is used to promote the nucleation of Ru nanocrystals, while thermal ALD is used to assist their growth. By the rigorous selection of each stage, we can demonstrate the formation of Ru nanocrystals with a density variation from 3.5×10^{11} to 8.4×10^{11} cm^{-2} and sizes from 2.2 to 5.1 nm, which is in the optimum density and size range of nanocrystal floating-gate memory application.
© 2008 The Electrochemical Society. [DOI: 10.1149/1.2952432] All rights reserved.

Manuscript submitted April 14, 2008; revised manuscript received May 12, 2008. Published July 11, 2008.

Nanocrystal (NC) floating-gate memory (NFGM) devices have been extensively investigated for the replacement of current flash memory devices, because a discrete NC layer provides charge-storage sites which are immune to stress-induced leakage through the tunnel oxide; thus, a relatively thin oxide can be used for the low-voltage operation.[1] In this type of device, it has been reported that the density and size of the NCs, as well as material types of the NC and the surrounding dielectrics, strongly affect device performance such as the threshold voltage shift (ΔV_{th}), charging efficiency, and charge retention time.[2-4] Theoretically, it has been reported that lower density and larger size of the NCs are favorable in the aspects of charging efficiency and retention characteristics.[2] At the same time, however, a reasonably high density of the NCs (up to 1×10^{12} cm^{-2}) is required in order to guarantee a sufficient memory window (conventionally 1–2 V difference of the ΔV_{th} before and after the NCs are charged). In addition, high density of the NCs is advantageous when the device size is as low as a few tens of nanometers because the deviation in the number of NCs per device can be statistically reduced.

Therefore, the density and size of the NCs should be rigorously controlled in order to obtain the optimum NFGM performance. However, independent control of the density and size is a very difficult task by employing any type of deposition processes such as physical vapor deposition (PVD) followed by thermal treatment,[5,6] chemical vapor deposition (CVD),[7-9] and atomic layer deposition (ALD).[10] For instance, in the case of a PVD-based process, in which many of the processes commonly have utilized thin-film agglomeration, density and size of the NCs are determined simultaneously by the nominal thickness of a starting film and the subsequent annealing temperature. In the case of CVD and ALD processes, the origin of these difficulties comes from the fact that the nucleation and growth occur simultaneously during the formation of the NCs. Thus, the density and size of NCs are determined only by deposition time at the given deposition conditions, including precursor injection time, partial pressure, and the type of substrate.

Certainly, one of the most promising ways to control density and size of NCs is to independently control the nucleation and growth stage during deposition. Ideally, it is hoped that the density of NCs is determined only by the nucleation stage, and the growth of these nuclei to the desirable size is controlled by the separated growth stage. A similar approach has been reported in the CVD-Si system using two different precursors of $SiCl_2H_2$ and SiH_4.[11] In their approach, Si NCs were nucleated by exposure of SiH_4 to the SiO_2 substrate and followed by selective growth of NCs using SiH_2Cl_2. They could deposit Si NCs with the narrower size distribution by the two-step method. However, they did not report on the independent control of the density and size. In our previous publication, we proposed an ALD process for the formation of NCs, because ALD provides more exact control of the supply of adatoms through repetition of the ALD cycles, which is based on the self-limiting surface-saturated reaction mechanism. In particular, nucleation in the ALD Ru was found to strongly depend on both the method of reducing the precursors and the surface state of the substrate.[10,12-14] In this article, we propose a method capable of producing Ru NCs with a tunable density and size using a two-step deposition process that combines plasma-enhanced ALD (PEALD) and thermal ALD in order to find out the optimum process window for density and size of NCs.

Ru NCs were deposited using a showerhead-type PEALD system at a temperature of 300°C and a pressure of 400 Pa. Ar was used as both a carrier and a purging gas. Diethylcyclopentadienyl ruthenium $[Ru(EtCp)_2]$ vapor was generated in a bubbler at 80°C and carried by Ar at a flow rate of 100 sccm. For the PEALD, radio frequency plasma of NH_3 was used as a reactant at a plasma power of 100 W. The flow rates of NH_3 during pulsing and Ar during purging were both 150 sccm. For the thermal ALD, the reactant was O_2 at a flow rate of 20 sccm. The pulsing sequences were $Ru(EtCp)_2$ pulsing, purging, reactant pulsing, and purging with durations of 5, 5, 15, and 3 s for the PEALD, and 5, 5, 10, and 5 s for the thermal ALD, respectively. Between PEALD and thermal ALD, we introduced an intermediate O_2 pulsing of 20 sccm for 500 s in order to suppress further nucleation. Thermally grown SiO_2 was used as a substrate for all of the processes. Detailed information about Ru ALD can be found elsewhere.[10,13] The spatial density, average size, and size distribution of the Ru NCs were measured using plan-view and cross-sectional transmission electron microscopy (TEM, JEOL JEM-3000F with a field emission gun operated at 300 kV).

We investigated the nucleation behavior of Ru deposited by PEALD and thermal ALD. As shown in Fig. 1, the PEALD process is quite effective in forming a high density of NCs, although the overall deposition rate is much lower. The data shows that the maximum density of the NCs obtained from PEALD is almost 50 times higher than that obtained from thermal ALD. More importantly, there is quite a difference in the size distribution of the NC array. There is a small variation in the size of NCs in PEALD, while thermal ALD induces a large variation. This result clearly demonstrates that the overall deposition process of PEALD occurs by the formation of a high density of NCs and the slow growth of them,

* Electrochemical Society Active Member.
[c] Present address: Semiconductor Business, Samsung Electronics Co., Ltd., Yongin, Gyeonggi-do 446-711, Korea.
[d] Present address: Samsung Advanced Institute of Technology, Suwon, Gyeonggi-do 440-600, Korea.
[z] E-mail: kibum@snu.ac.kr

Downloaded 14 Jul 2008 to 147.46.136.237. Redistribution subject to ECS license or copyright; see http://www.ecsdl.org/terms_use.jsp

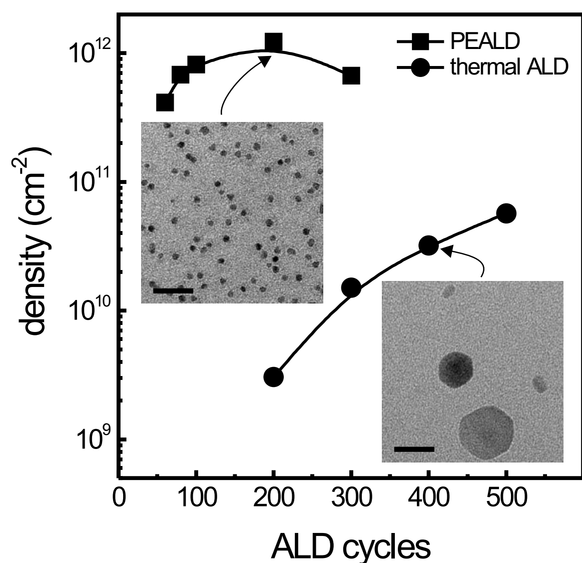

Figure 1. Density of the Ru NC deposited by PEALD (square symbols) and thermal ALD (circle symbols). Inset figures are plan-view bright-field TEM micrographs of the Ru NCs deposited by PEALD for 200 ALD cycles (left) and thermal ALD for 400 ALD cycles (right). Scale bars in the micrographs correspond to 20 nm.

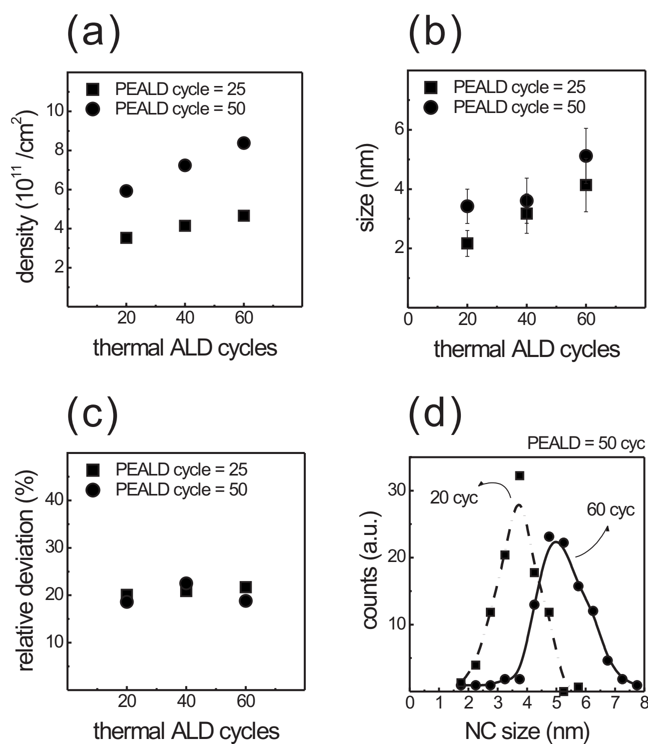

Figure 3. (a) Density, (b) size, (c) relative standard deviation of size, and (d) size distribution of the Ru NCs deposited by the two-step process. Square symbols in (a), (b), and (c) represent the NCs with PEALD cycles of 25 and circle symbols for the NCs with 50 PEALD cycles. Square symbols in (d) correspond to thermal ALD growth cycles of 20 and circle symbols 60 with the same PEALD nucleation cycles of 50. Each data point in (d) represents the total number of NCs having a size between $0.5n$ and $0.5(n + 1)$ nm, where n is an integer.

while the thermal ALD proceeds by the low nucleation rate and the fast growth. Based on these results of two ALD processes, we tried to control the density of NCs by using PEALD and the size of them by using thermal ALD.

As a two-step deposition process, we performed the PEALD for 25 and 50 cycles as a nucleation stage followed by thermal ALD for 20, 40, and 60 cycles as a growth stage. Figure 2 shows plan-view bright-field TEM micrographs of the Ru NCs deposited by a two-step process. It was found that the Ru NCs with a spherical shape and uniform size are formed on the surface. Although the main growth process is the thermal ALD, the resulting size variation of the NCs resembles that of PEALD (left inset of Fig. 1) rather than the thermal ALD (right inset of Fig. 1). At the same number of the thermal ALD cycles, the average sizes with the PEALD nucleation cycles of 50 are approximately 1 nm larger than those with 25 PEALD cycles due to the difference in the starting size of the NCs before the growth stage.

Figure 3a shows the spatial density of the Ru NCs as a function of the number of thermal ALD cycles measured from plan-view

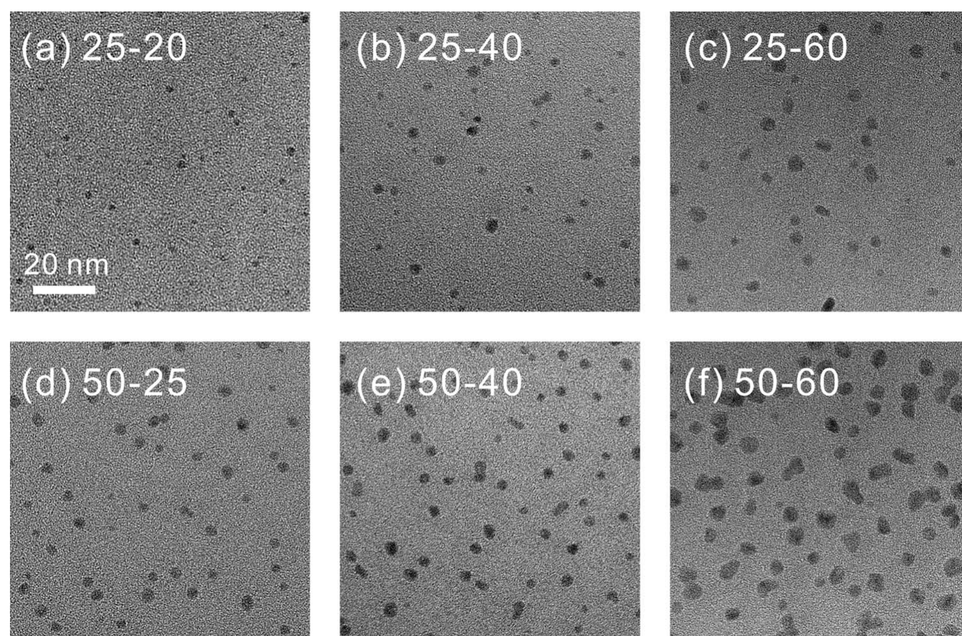

Figure 2. Bright-field TEM micrographs of the Ru NC deposited by the two-step process. The number of PEALD–thermal ALD cycles is (a) 25–20, (b) 25–40, (c) 25–60, (d) 50–20, (e) 50–40, and (f) 50–60. Scales of all of micrographs are the same as (a).

Downloaded 14 Jul 2008 to 147.46.136.237. Redistribution subject to ECS license or copyright; see http://www.ecsdl.org/terms_use.jsp

high-resolution TEM (HRTEM) images. The density increases linearly with increasing number of thermal ALD cycles in both cases of the PEALD nucleation cycles. Our intention is to suppress the additional nucleation during growth stages, but approximately 30 and 40% of the additional nucleation occurred in the case of PEALD nucleation cycles of 25 and 50, respectively. We suggest two possible explanations for this. We introduced intermediate O_2 pulsing in order to suppress the additional nucleation by oxidizing the surface of the substrate, because the nucleation in PEALD is thought to be enhanced by the NH_3 plasma nitridation of the oxide surface.[13] Thus, the additional nucleation can occur due to the limited oxidation of the nitrided surface. Here, we note that the intermediate O_2 pulsing does not cause the oxidation of Ru NCs, which was confirmed by X-ray diffractometry and HRTEM. In addition, the additional nucleation can originate from the experimental limitation. The NCs with a size of less than 1 nm are difficult to observe even in the HRTEM. Thus, the invisible NCs at the low thermal ALD cycles may appear as larger NCs after they go through the subsequent growth. This suggestion is supported by Fig. 3d. In the case of the Ru NCs with 50 PEALD cycles followed by 60 thermal ALD cycles, few NCs with the size of less than 3 nm are found, which implies that the additional nucleation, in fact, might not be significant.

We also measured the size, relative size deviation, and size distribution of the NCs from the HRTEM, as shown in Fig. 3b-d. The relative standard deviation of the size in Fig. 3c is defined as a standard deviation of size divided by an average size. Figure 3b shows that the growth of the Ru NCs has linearity with the thermal ALD cycles. In addition, Fig. 3d shows that the NCs grow maintaining the shape of the distribution curves, while the width of the distribution curves increases slightly, which is related to the increase in the absolute value of the standard deviation of the size of the NCs. As shown in Fig. 3c, the relative deviations of all the samples lie near 20%. The size deviation of 20%, obtained by the two-step ALD process, is significantly lower than that by one-step deposition such as thermal ALD ($>60\%$). This also implies that the size distributions, as well as the density and size, can be tightly controlled by the present method.

We further estimated the process window with respect to the density and size of NCs which can be obtained from the two-step deposition process in Fig. 4. For all of the PEALD cycles, the average size has a linear relationship with the density within the range of error. Thus, the density and size on the solid line in Fig. 4 can be obtained by adjusting the number of thermal ALD cycles at each PEALD cycle. In Fig. 4, the lower bound (dashed line) is obtained from the results of the one-step PEALD process. The upper bound (dotted line) is theoretical limitation of the maximum size of NCs calculated at the given density and packing order. For instance, if the density of the Ru NCs is set to be n, the maximum average size, d, is limited by the following inequality

$$n < \frac{A}{(d + a)^2} \quad [1]$$

where a is spacing between the edges of the adjacent NCs at the maximum density and constant, and A is a geometric factor that is related with the packing state of the NCs. The value of A is $4/\sqrt{3}$ when the array of the NCs has the two-dimensional hexagonal packing, as indicated in the inset of Fig. 4. We obtained a value of A and a of 0.53 and 3.2 nm, respectively, from the density and size of the NCs deposited by the PEALD for 200 cycles and by the two-step process with PEALD/thermal ALD cycles of 50/60, which are regarded as the condition giving the maximum density and size. Based on this analysis, it is expected that the Ru NCs with a density from 4×10^{11} to 6×10^{11} cm^{-2} and size from 2 to 6 nm can be deposited when the PEALD for 25 cycles is used as a nucleation stage.

In summary, we deposited the Ru NCs with controllable size and density by a two-step process. PEALD is used as the nucleation process, which provides high density and small size of the Ru NCs, while thermal ALD is used as a growth process. By the present method, the NCs with a wide range of density and size can be deposited with a narrow size distribution, which provides the groundwork for studying the effects of density and size of NCs on the performance of NFGMs.

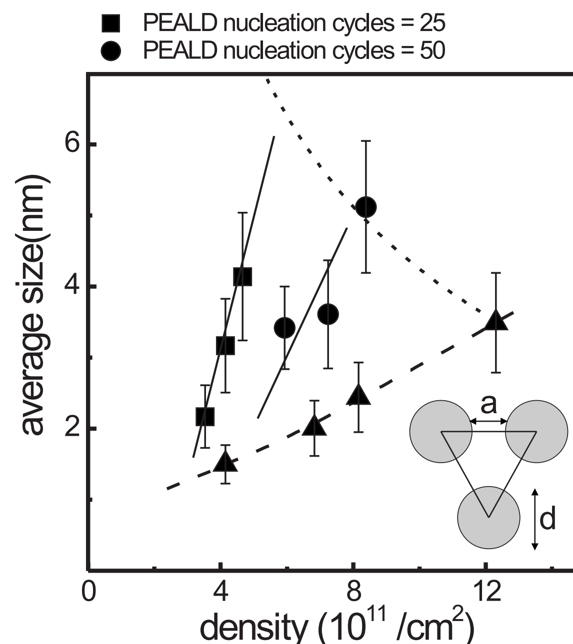

Figure 4. Process window for the available density and size that can be deposited by the present deposition method. Triangle symbols represent the density and size of the NCs deposited by the one-step PEALD process for 60, 80, 100, and 200 cycles (from left to right). Square and circle symbols indicate a two-step process using the PEALD nucleation cycles of 25 and 50, respectively. In both cases, thermal ALD cycles are sequentially 20, 40, and 60 (from left to right). Inset shows the example of hexagonally packed NCs with a diameter d and adjacent spacing a.

Acknowledgment

This work was supported by the National Program for Tera-Level Nano Devices, one of the Frontier R&D Programs funded by the Korean Ministry of Science and Technology. We also acknowledge that part of the funding came from the BK-21 program through the Ministry of Education of Korea.

Seoul National University assisted in meeting the publication costs of this article.

References

1. A. Thean and J.-P. Leburton, *IEEE Potentials*, **21**, 35 (2002).
2. T.-H. Hou, C. Lee, V. Narayana, U. Ganguly, and E. C. Kan, *IEEE Electron Device Lett.*, **53**, 3095 (2006).
3. T.-H. Hou, C. Lee, V. Narayana, U. Ganguly, and E. C. Kan, *IEEE Electron Device Lett.*, **53**, 3103 (2006).
4. B. DeSalvo, G. Ghibaudo, G. Pananakis, P. Masson, T. Baron, N. Buffet, A. Fernandes, and B. Guillaumot, *IEEE Trans. Electron Devices*, **48**, 1789 (2001).
5. Z. Liu, C. Lee, V. Narayanan, G. Pei, and E. C. Kan, *IEEE Trans. Electron Devices*, **49**, 1606 (2002).
6. J. J. Lee, Y. Harada, J. W. Pyun, and D.-L. Kwong, *Appl. Phys. Lett.*, **86**, 103505 (2005).
7. R. Muralidhar, R. F. Steimle, M. Sadd, R. Rao, C. T. Swift, E. J. Prinz, J. Yater, L. Grieve, K. Harber, B. Hradsky, et al., *Tech. Dig. - Int. Electron Devices Meet.*, **2003**, 26.2.1.
8. S. J. Baik, S. Choi, U.-I. Chung, and J. T. Moon, *Tech. Dig. - Int. Electron Devices Meet.*, **2003**, 22.3.1.
9. B. De Salvo, C. Gerardi, S. Lombardo, T. Baron, L. Perniola, D. Mariolle, P. Mur, A. Toffoli, M. Gely, M. N. Semeria, et al., *Tech. Dig. - Int. Electron Devices Meet.*, **2003**, 26.1.1.

Downloaded 14 Jul 2008 to 147.46.136.237. Redistribution subject to ECS license or copyright; see http://www.ecsdl.org/terms_use.jsp

10. S.-S. Yim, M.-S. Lee, K.-S. Kim, and K.-B. Kim, *Appl. Phys. Lett.*, **89**, 093115 (2006).
11. F. Mazen, T. Baron, A. M. Papon, R. Truche, and J. M. Hartmann, *Appl. Surf. Sci.*, **214**, 359 (2003).
12. O.-K. Kwon, S.-H. Kwon, H.-S. Park, and S.-W. Kang, *J. Electrochem. Soc.*, **151**, C753 (2004).
13. S.-S. Yim, D.-J. Lee, K.-S. Kim, K.-B. Kim, S.-H. Kim, and T.-S. Yoon, *J. Appl. Phys.*, **103**, 113509 (2008)
14. K. J. Park, D. B. Terry, S. M. Stewart, and G. N. Parsons, *Langmuir*, **23**, 6106 (2007).

Downloaded 14 Jul 2008 to 147.46.136.237. Redistribution subject to ECS license or copyright; see http://www.ecsdl.org/terms_use.jsp